

# Net1 Stimulates RNA Polymerase I Transcription and Regulates Nucleolar Structure Independently of Controlling Mitotic Exit

Wenying Shou,<sup>1</sup> Kathleen M. Sakamoto,<sup>1,6</sup> John Keener,<sup>3</sup> Kenji W. Morimoto,<sup>3</sup> Edwin E. Traverso,<sup>5</sup> Ramzi Azzam,<sup>1</sup> Georg J. Hoppe,<sup>4,7</sup> R.M. Renny Feldman,<sup>1</sup> John DeModena,<sup>1</sup> Danesh Moazed,<sup>4</sup> Harry Charbonneau,<sup>5</sup> Masayasu Nomura,<sup>3</sup> and Raymond J. Deshaies<sup>1,2,9</sup>

<sup>1</sup>Division of Biology

<sup>2</sup>Howard Hughes Medical Institute  
California Institute of Technology  
Pasadena, California 91125

<sup>3</sup>Department of Biological Chemistry  
University of California, Irvine  
Irvine, California 92697

<sup>4</sup>Department of Cell Biology  
Harvard Medical School  
240 Longwood Avenue  
Boston, Massachusetts 02115

<sup>5</sup>Department of Biochemistry  
Purdue University  
West Lafayette, Indiana 47907-1153

<sup>6</sup>Department of Pediatrics and Pathology  
Division of Hematology-Oncology  
UCLA School of Medicine and Jonsson Comprehensive  
Cancer Center

Los Angeles, California 90095

<sup>7</sup>FB Biologie

Chemie  
Pharmazie  
Freie Universität Berlin  
14195 Berlin  
Germany

<sup>8</sup>Department of Biology  
Pomona College  
Claremont, California 91711

## Summary

The budding yeast RENT complex, consisting of at least three proteins (Net1, Cdc14, Sir2), is anchored to the nucleolus by Net1. RENT controls mitotic exit, nucleolar silencing, and nucleolar localization of Nop1. Here, we report two new functions of Net1. First, Net1 directly binds Pol I and stimulates rRNA synthesis both *in vitro* and *in vivo*. Second, Net1 modulates nucleolar structure by regulating rDNA morphology and proper localization of multiple nucleolar antigens, including Pol I. Importantly, we show that the nucleolar and previously described cell cycle functions of the RENT complex can be uncoupled by a dominant mutant allele of *CDC14*. The independent functions of Net1 link a key event in the cell cycle to nucleolar processes that are fundamental to cell growth.

## Introduction

Unexpected links between the nucleolus and the cell cycle have been uncovered (reviewed by Garcia and Pillus, 1999; Cockell and Gasser, 1999).

In the budding yeast *Saccharomyces cerevisiae*, the RENT protein complex regulates mitotic exit, nucleolar silencing, and Nop1 localization through its three known components: Cdc14, Sir2, and Net1 (also known as Cfi1; Shou et al., 1999; Straight et al., 1999; Visintin et al., 1999).

The yeast nucleolus, which contains ~150 consecutive repeats of the rDNA, is the center for ribosomal RNA synthesis and ribosome assembly (reviewed in Shaw and Jordan, 1995). The chromatin structure in the nucleolus silences transcription by RNA polymerase II without interfering with highly active transcription by RNA polymerase I (Pol I; reviewed in Guarente, 2000). This restriction, termed “nucleolar silencing,” may be the consequence of a mechanism that evolved to suppress recombination among rDNA repeats and thereby may reduce the production of rDNA circles that have been shown to cause cellular senescence (reviewed in Guarente, 2000). The RENT complex, tethered to the nucleolus by its core subunit Net1, influences the nucleolus in at least two ways. First, both Net1 and Sir2 are essential for nucleolar silencing, and Net1 influences rDNA chromatin in part by tethering Sir2 to the nucleolus (Straight et al., 1999). Sir2 in turn mediates silencing, suppression of recombination, and extension of longevity through its NAD-dependent histone deacetylase activity (reviewed by Gottschling, 2000; Guarente, 2000) and/or other mechanisms such as NAD breakdown and generation of O-acetyl-ADP-ribose (Tanner et al., 2000; Tanny and Moazed, 2000). Second, Net1 is required to maintain nucleolar localization of Nop1 (Straight et al., 1999), a protein implicated in pre-rRNA processing, methylation, and ribosome assembly (Tollervey et al., 1993). It is not known whether defective localization of Nop1 in *net1* cells is specific or whether it results from a general perturbation of nucleolar structure. Despite the key role of the nucleolus in cellular metabolism, the molecular basis for nucleolar assembly/organization and the role of Net1 in this process remain mysterious.

Besides its role in nucleolar processes, the RENT complex also controls mitotic exit. When cells exit mitosis, the mitotic exit network (MEN) triggers accumulation of the Cdk inhibitor Sic1 and degradation of B-type mitotic cyclins (Clbs) and consequently inactivation of mitotic Cdc28 (reviewed by Zachariae and Nasmyth, 1999). Members of the MEN include Tem1 (a GTP binding protein), Lte1 (a putative guanine nucleotide releasing factor), Cdc14 (a protein phosphatase), Cdc15 (a kinase), Dbf2/Dbf20 (kinases), Cdc5 (a kinase), Mob1 (a protein that binds to Dbf2), and Nud1 (reviewed in Morgan, 1999; Gruneberg et al., 2000). When cells harboring conditional-lethal temperature sensitive (ts) mutations in any of the MEN genes are shifted to the restrictive temperature, they uniformly arrest in late anaphase as large-budded cells with segregated chromosomes, elongated spindles, and in all tested cases, elevated Cdc28 activity.

To address how the MEN is organized and regulated, we previously sought *telophase arrest bypassed* (*tab*) mutants that alleviate the essential requirement for *CDC15* and *TEM1*. One of these mutants, *tab2-1* (*net1-1*), enabled

<sup>9</sup>Correspondence: deshaies@its.caltech.edu

Cib2 degradation and Sic1 accumulation even in the absence of Tem1 (Shou et al., 1999). Further characterization of Net1 led us and others to propose the “RENT control” hypothesis: Throughout most of the cell cycle, Net1 sequesters Cdc14 in the nucleolus and inhibits its phosphatase activity. As cells exit mitosis, a *TEM1/CDC15*-dependent signal leads to disassembly of the RENT complex, causing Cdc14 and Sir2 to vacate the nucleolus (Shou et al., 1999; Straight et al., 1999; Visintin et al., 1999). The evicted Cdc14 subsequently catalyzes Cdc28 inactivation (Visintin et al., 1998; Jaspersen et al., 1999). However, it is unknown whether release of Cdc14 from the nucleolus is sufficient to bypass *cdc15Δ* and *tem1Δ*.

In this study, we describe new functions of Net1 in the nucleolus: It directly activates synthesis of rRNA by RNA Pol I and plays a general role in regulating nucleolar structure. The perturbed nucleolar structure in *net1-1* cells raises the possibility that mislocalized nucleolar proteins other than Cdc14 could cause or contribute to the *cdc15Δ* bypass phenotype. Characterization of a second *tab* locus, *TAB6-1*, proves this possibility unlikely and provides key support to the RENT control hypothesis. *TAB6-1* is a dominant allele of *CDC14* that bypasses *cdc15Δ* and *tem1Δ* without perturbing nucleolar structure or Pol I function. Thus, the release of Cdc14 from the nucleolus is sufficient to trigger mitotic exit in the absence of MEN proteins, and the role of RENT in cell cycle control can be uncoupled from its roles in maintenance of nucleolar integrity and Pol I transcription.

## Results

### *RRN3* Suppresses Temperature Sensitivity of *net1* Mutants

*NET1* has been implicated in three potentially distinct cellular processes: mitotic exit, nucleolar silencing, and proper localization of the nucleolar antigen Nop1 (Shou et al., 1999; Straight et al., 1999; Visintin et al., 1999). *net1-1* cells grow slowly, and *net1Δ* cells fail to grow at 37°C, which could result from improper mitosis, an abnormal nucleolus, or defects in some other unknown functions of *NET1*. To distinguish between these possibilities, we screened a CEN/ARS-based yeast genomic library to identify genes that rescued the ts growth defect of *net1-1*. In addition to *NET1*, this effort yielded *RRN3* (Figure 1A; see Experimental Procedures), a transcription activator for RNA Pol I (Yamamoto et al., 1996). Strikingly, centromeric plasmids containing *NET1* (*[NET1]*) or *RRN3* (*[RRN3]*) driven by their respective native promoters rescued the temperature sensitivity of *net1Δ* to similar extents (Figure 1B). The level of Rrn3 protein in *net1* mutants was not diminished at 25°C or 37°C (Figure 1C), suggesting that the ts growth defects of *net1* mutants did not result from reduced amounts of Rrn3.

It is unlikely that *RRN3* suppressed the growth defect of *net1* mutants by restoring nucleolar silencing because a lack of silencing in *sir2Δ* does not affect growth. It is also unlikely that suppression involved mitotic exit, since in the presence of *[RRN3]*, *net1-1* still bypassed *cdc15Δ* (W.S., data not shown). Nop1, a protein involved

in pre-rRNA processing and ribosome assembly, is delocalized from the nucleolus in *net1Δ* cells (Straight et al., 1999). Although it is not known whether delocalization of Nop1 impedes cell growth, we tested whether the *RRN3* plasmid affected Nop1 localization in *net1* mutants. Whereas Nop1 assumed a characteristic nucleolar localization pattern (a crescent-shaped structure abutting the nucleus) in 98% of wild-type cells, only 17% of *net1-1* cells showed a significant or complete Nop1 localization to the nucleolus at 37°C (Figure 1D). However, this fraction was increased to 64% by the *RRN3* plasmid (Figure 1D). Similarly, the fraction of cells with significant or complete localization of Nop1 to the nucleolus was increased from 9% in *net1Δ* to 46% in *net1Δ* *[RRN3]* at 25°C (Figure 1D). Thus, *RRN3* on a centromeric plasmid partially restored correct Nop1 localization in *net1* mutants, suggesting that the growth defect of these mutants arose from a disruption of nucleolar structure and function.

### rRNA Synthesis Is Reduced in *net1-1*

Given that extra Rrn3, a transcription factor for Pol I, suppressed the ts growth defect of *net1* mutants, a key function of Net1 might be to sustain Pol I activity. To test this hypothesis, we evaluated rRNA and actin mRNA accumulation in *net1-1* mutants by ethidium bromide staining and Northern blotting, respectively. The level of rRNA in *net1-1* cells at 37°C, normalized to actin mRNA, was reduced by ~40% compared with that in wild-type cells (Figure 2A).

The reduced level of rRNA in *net1-1* could result from a reduced rate of transcription or defective processing of pre-rRNA. To distinguish between these possibilities, we performed pulse-chase experiments using [<sup>3</sup>H]-methionine, which has the advantage of being rapidly incorporated into rRNA through methylation and even more rapidly chased (Warner, 1991). *net1* mutants did not exhibit a major defect in 35S, 27S, and 20S pre-rRNA processing (Figure 2B, lower panel). However, the *net1* mutants incorporated much less [<sup>3</sup>H]-methionine (Figure 2B, lower panel; note the 7-fold longer exposure time for *net1Δ*), which could result from reduced rRNA methylation or transcription. We therefore repeated the pulse-chase experiment using [<sup>3</sup>H]-uracil and adjusted exposure time such that the labeling of tRNA (synthesized by Pol III) was approximately equivalent. In *net1* mutants, mature 25S and 18S rRNA transcripts were produced at a slower rate (Figures 2C, lower panel, and 2D). We suggest that the large difference in rate of appearance of mature rRNA in wild-type versus *net1* cells is due to changes in the actual rate of transcription by Pol I and not due simply to changes in nucleotide pool sizes. Curiously, the *net1Δ* cells analyzed in this experiment displayed a less severe defect in rRNA synthesis than the *net1-1* cells. In our experience, the slow-growth phenotype of *net1Δ* cells was neither uniform nor stable: The two *net1Δ* spores from a single tetrad frequently displayed unequal growth rates, and upon subculturing, *net1Δ* cells always began to grow faster (W.S., data not shown). Thus, it is possible that *net1Δ* cells accumulated second site mutations more efficiently than *net1-1* or acquired more rDNA repeats through mitotic recombination to compensate for the severe reduction in rRNA

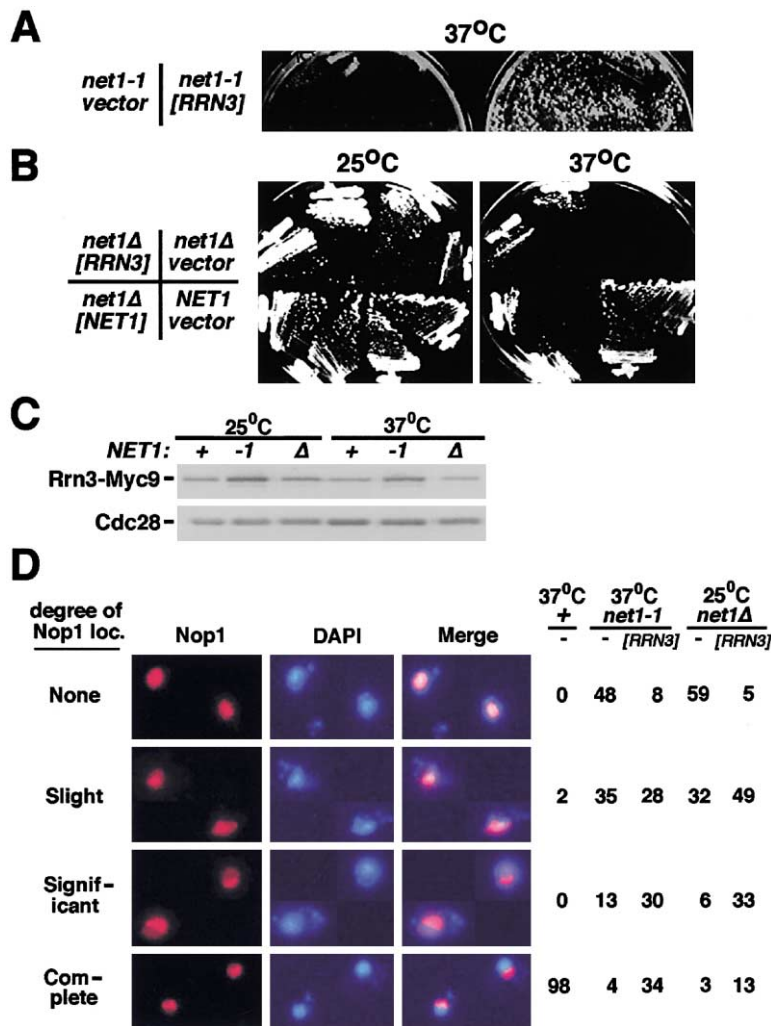


Figure 1. A CEN/ARS Plasmid Containing *RRN3* ([RRN3]) Suppresses the Temperature-Sensitive (ts) Growth Defect and Nop1 Mislocalization Phenotype of *net1* Mutants

(A and B) [RRN3] suppresses *net1* ts growth defect. (A) *net1-1* cells transformed with a CEN/ARS/LEU2 plasmid harboring either no insert (vector) or *RRN3* under its natural promoter were plated onto synthetic dextrose medium lacking leucine. After 25°C for one day, both plates were shifted to 37°C for two more days, and then photographed. (B) *NET1* and *net1Δ* cells transformed with a CEN/ARS/LEU2 plasmid harboring either no insert (vector), *RRN3* or *NET1* (driven by their natural promoters) were streaked onto synthetic dextrose medium lacking leucine. Two independent colonies were analyzed in each case. The plates were photographed after four days at 25°C or five days at 37°C.

(C) Wild-type and *net1* mutants were pre-grown at 25°C to exponential phase and shifted to 25°C or 37°C for three more hours. Extracts were fractionated by SDS-PAGE and immunoblotted with 9E10 antibodies (against the Myc epitope) to measure the level of Rrn3-Myc9. Cdc28 served as a loading control.

(D) [RRN3] partially restores Nop1 nucleolar localization in *net1* mutants. Wild-type and *net1* mutants with or without [RRN3] plasmid were grown at 25°C to exponential phase. Some cultures were further incubated at 37°C for 3 hr as indicated. Cells were subjected to indirect immunofluorescence with anti-Nop1, and the extent of Nop1 delocalization in *net1* mutants was categorized into four classes: none, complete delocalization such that Nop1 staining is uniform across the entire nucleus; slight, strong nuclear staining with stronger nucleolar staining; significant, intense nucleolar staining and subdued nuclear staining; and complete, nucleolar localization with no detectable nuclear staining. Fractions of cells that fell in the four different classes were quantitated.

synthesis. In addition to a reduced rate of rRNA synthesis, subtle defects in rRNA processing were evident in *net1* cells: 27S pre-rRNA persisted longer in *net1-1*, and an aberrant band appeared above 25S rRNA at later time points in both *net1* mutants (Figure 2C). However, the abundance of the processing intermediates was low compared with that of mature rRNA products. Thus, both *net1Δ* and *net1-1* mutants exhibit a major defect in rRNA synthesis, but not processing.

**Net1 Retains the A190 Subunit of Pol I in the Nucleolus**  
Reduced transcription of rRNA is indicative of diminished activity of the Pol I transcriptional machinery in *net1* mutants, which could result from reduced protein levels, mislocalization, or inactivity of Pol I itself. Whereas the level of A190 was slightly reduced in *net1Δ*, it was normal in *net1-1* cells (Figure 3E, top panel), suggesting that although Net1 helps to sustain normal levels of Pol I, Pol I levels alone cannot account for the reduced rRNA transcription in *net1-1*. Next, we probed for the localization of A190 by indirect immunofluorescence. Whereas A190 displayed a characteristic nucleolar

staining pattern in wild-type cells, it was partially delocalized in *net1-1* and *net1Δ* mutants (Figure 3A).

Because Net1 was required for the proper localization of both A190 and Nop1, we asked whether Net1 physically associates with them. Extract prepared from MYC9-NET1 cells was purified on 9E10 antibody resins, and bound proteins were detected by immunoblotting. Besides Sir2 (data not shown; Straight et al., 1999), A190 but not Nop1 was specifically recovered in association with Myc9-Net1 (Figure 4A, lanes 3 and 4). Mass spectrometry-based sequencing of Net1-associated proteins confirmed that other subunits of Pol I coimmunoprecipitated with Net1, suggesting that Net1 binds the intact Pol I holoenzyme (R.A. and A. Shevchenko, unpublished data).

To determine whether Net1 binds directly to Pol I, we attempted to reconstitute the association of these proteins in vitro. His6-Myc9-Net1 was expressed in insect cells and was purified on a nickel affinity column. The purified protein was functional because it bound GST-Sir2 (Figure 4B) and GST-Cdc14 (R.A. and W.S., data not shown). Hemagglutinin (HA) epitope-tagged,

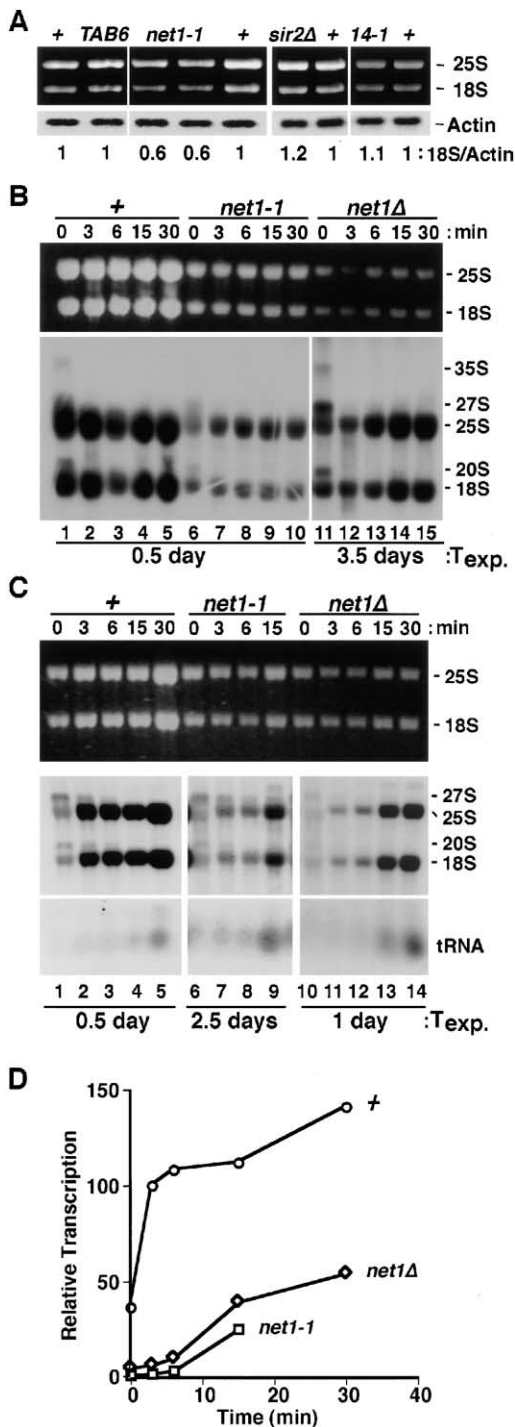


**Figure 2. *net1* Mutants Have a Reduced Rate of rRNA Synthesis**  
(A) The steady-state level of rRNA is reduced in *net1-1*. Total RNA was extracted from cells grown at 23°C and shifted to 37°C for three hours. Equal amounts of total RNA were separated by agarose gel electrophoresis, first stained with ethidium bromide to show the levels of 25S and 18S rRNA (upper panel), and then probed for actin mRNA in a Northern blot (lower panel). The ratio of 18S rRNA to actin mRNA is shown below each lane.  
(B–D) *net1* mutants have almost normal rRNA processing but reduced rRNA transcription. Cells were grown at 25°C, shifted to 37°C for 3 hr, and kept at 37°C thereafter. They were pulse-labeled with [<sup>3</sup>H]-methionine (B) or [<sup>3</sup>H]-uracil (C) for 5 min and chased with unlabeled methionine (B) or uracil (C) for 0, 3, 6, 15, or 30 min, as

purified Pol I complexes also efficiently captured His6-Myc9-Net1 (Figure 4C, lanes 3 and 4). This observation indicates that Pol I bound directly to the Net1 subunit of RENT.

#### Net1 Stimulates Pol I Activity In Vitro

To test whether Net1 could directly activate Pol I, lysates from insect cells either mock infected or infected with a baculovirus that expressed His6-Myc9-Net1 were adsorbed to nickel-NTA resin, and specifically bound proteins were eluted and added to a standard transcription reaction that contained linearized rDNA template, Pol I, Rrn3, TATA binding protein (TBP), upstream activating factor (UAF), and core factor (CF; Keener et al., 1998). His6-Myc9-Net1 stimulated rRNA synthesis 2.2-fold relative to the mock sample (Figure 5A). To confirm Net1's stimulatory effect, we repeated this experiment with His6-Myc9-Net1 that was further enriched on SP- and Q-sepharose columns, resulting in a preparation with >90% purity (Figure 5B). The production of [<sup>32</sup>P]-labeled runoff transcripts (arrow in Figure 5C) increased as a function of input Net1 (Figures 5C and 5D), with the maximum stimulation being slightly more than 4-fold. Furthermore, maximum stimulation occurred at a concentration of Net1 that was approximately equimolar with Pol I, suggesting that Net1 stimulates Pol I transcription by helping to recruit Pol I to the rDNA templates present in our in vitro reactions. Taken together, our data indicate that Net1 is required for optimal activity of Pol I, both in vivo and in vitro.

#### Nucleolar Structure Is Perturbed in *net1* Mutants

The failure of Cdc14, Sir2, and Pol I to localize properly to the nucleolus in *net1Δ* (Shou et al., 1999; Straight et al., 1999; Visintin et al., 1999; Figure 3A) could be explained by the fact that they all directly bound Net1 (Traverso et al., 2001; Figures 4B and 4C). In contrast, delocalization of Nop1 in *net1* mutants (Figure 3B) is harder to explain given that Nop1 did not stably associate with Net1 (Figure 4A). The simplest model predicts that Net1 directly or indirectly influenced nucleolar structure, which in turn dictated the localization pattern of Nop1 and possibly other nucleolar proteins.

To test this model, we examined the localization patterns of two additional nucleolar proteins in various mutants. Nop2 (de Beus et al., 1994) exhibited a nucleolar staining pattern in wild-type and *net1-1* but not *net1Δ* cells (Figure 3C, top three rows). Mislocalization of Nop2 in *net1Δ* was not due to increased levels of this protein (Figure 3E, bottom panel). In contrast, the localization pattern of Fpr3 (Benton et al., 1994) was altered in a different way in both *net1* mutants: Despite near equivalent levels of Fpr3 in all strains examined (Figure 3E, bottom panel), the staining area of Fpr3 appeared to be smaller in *net1* mutants than in wild-type cells (Figure 3D, compare rows 2 and 3 with row 1).

indicated. Total RNA was separated by agarose gel electrophoresis, stained with ethidium bromide (upper panel), and subjected to autoradiography for the indicated amounts of time ( $T_{exp}$ ) (lower panel). The amount of the [<sup>3</sup>H]-uracil-labeled 25S rRNA from equivalent OD<sub>600</sub> cells was quantitated and plotted in (D).

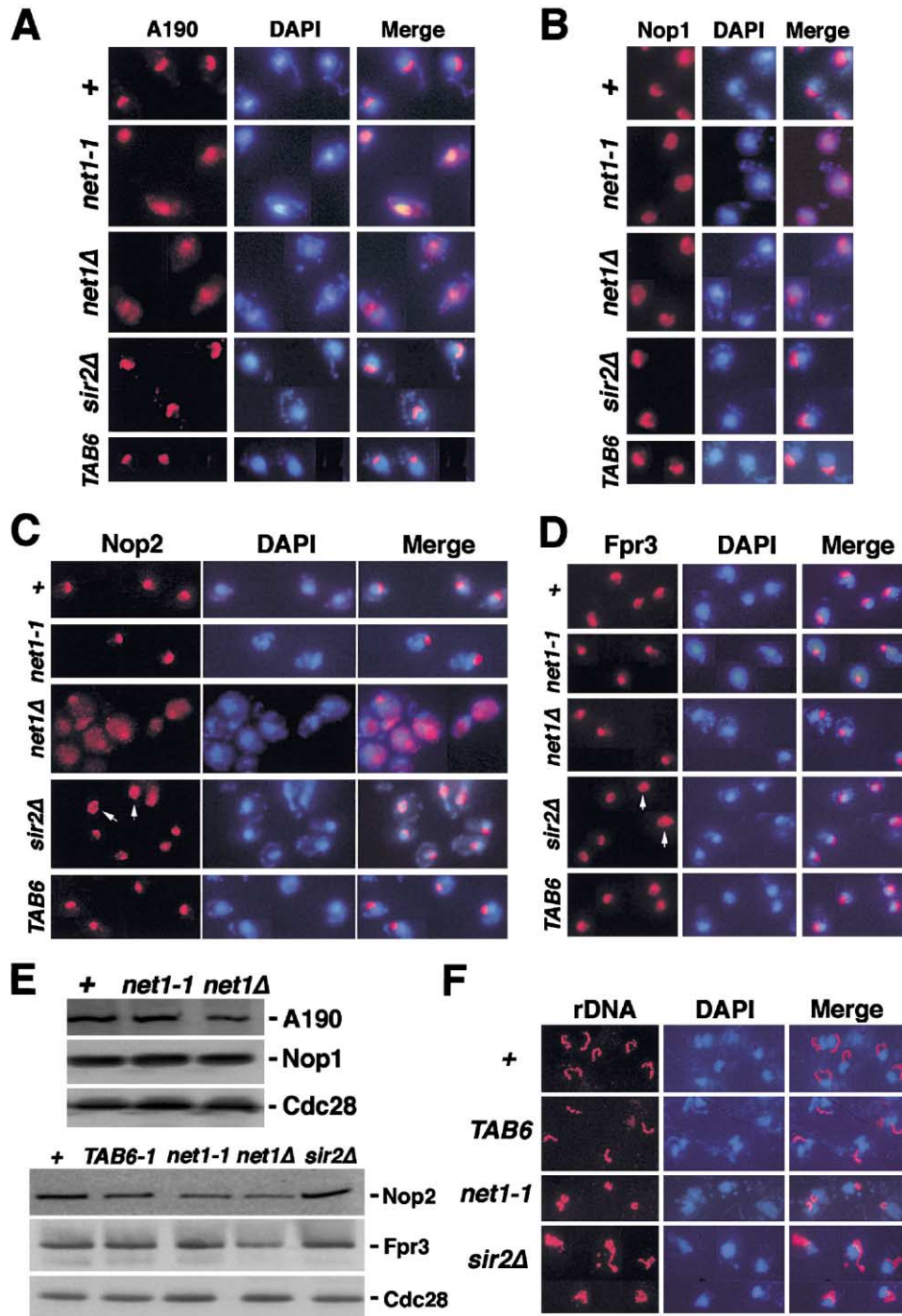


Figure 3. Net1 Is Required for the Proper Localization of Multiple Nucleolar Proteins

(A–D) Cells with indicated genotypes were grown at 25°C and subjected to indirect immunofluorescence with anti-A190 (A), anti-Nop1 (B), anti-Nop2 (C), or anti-Fpr3 (D) antibodies (column 1). They were also stained with DAPI to show the position of nuclei (column 2). The images in columns 1 and 2 were merged in column 3. In 40%–50% of *sir2Δ* and 20% of wild-type cells, Nop2 and Fpr3 assumed diffused staining patterns that covered the majority of the nucleus or even exceeded the boundary of the nucleus (white arrows in panels C and D).

(E) Protein levels of the four nucleolar antigens in wild-type and mutant cells were compared in Western blots, with Cdc28 serving as the loading control.

(F) rDNA morphology is altered in *net1* and *sir2* but not *TAB6-1* mutants. Cells were arrested in nocodazole and subjected to fluorescence in situ hybridization (FISH) using DIG-labeled probes against rDNA followed by rhodamine-anti-DIG (column 1). DNA was visualized by DAPI staining (column 2). The merged image is shown in column 3.

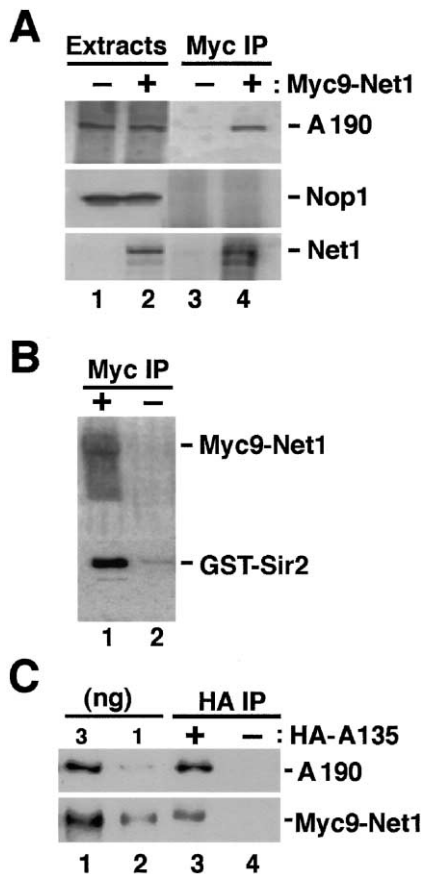


Figure 4. Pol I but Not Nop1 Binds Stably to Net1

(A) A190 but not Nop1 binds stably to Net1. Extracts from strains with the indicated genotypes were immunoprecipitated with 9E10 antibodies ("-" refers to a strain with a natural [that is, untagged] *NET1* allele). The immunoprecipitates (Myc IP) and the input extracts were fractionated by SDS-PAGE and immunoblotted with antibodies against A190 (first row), Nop1 (second row), and Myc9-Net1 (third row).

(B) His6-Myc9-Net1 and GST-Sir2 interact in vitro. His6-Myc9-Net1 and GST-Sir2 were expressed and purified from insect cells and bacteria, respectively. 9E10 antibody beads were incubated with GST-Sir2 in the presence (+) or absence (-) of Myc9-Net1. Proteins captured by the beads were immunoblotted with 9E10 and  $\alpha$ -GST antibodies.

(C) Purified Pol I and Myc9-Net1 interact in vitro. Purified Pol I (150 ng = 0.26 pmol; Keener et al., 1998) with its A135 subunit tagged with HA (+) or untagged (-) was immunoprecipitated with 12CA5 antibodies (against the HA epitope). The antibody beads were subsequently incubated with Myc9-Net1 (150 ng = 0.83 pmol) purified from insect cells, and proteins bound to the beads (lanes 3 and 4) were immunoblotted with antibodies against A190 and Myc9-Net1. To estimate the relative amount of Net1 complexed to Pol I, 3 ng (lane 1) and 1 ng (lane 2) of Pol I (top panel) and Myc9-Net1 (bottom panel) were immunoblotted with anti-A190 and 9E10 antibodies, respectively. We estimate that almost all Pol I molecules bound Net1 in this assay.

The abnormal localization patterns of most nucleolar proteins examined so far in *net1* mutants led us to examine whether the organization of rDNA itself was perturbed in these cells. Cells were arrested in mitosis with nocodazole and subjected to fluorescence in situ hybridization (FISH; Guacci et al., 1994). Whereas wild-type cells displayed line-shaped rDNA that appeared to be spooled away from the focus of 4',6-diamidino-2-

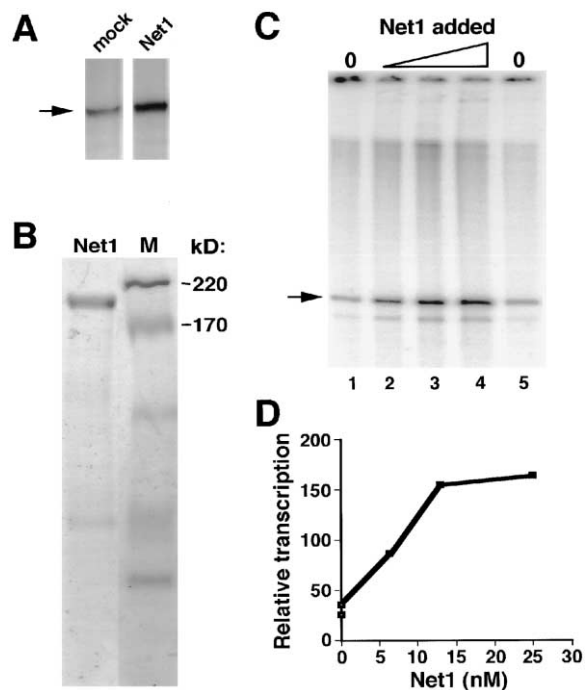


Figure 5. Net1 Stimulates Pol I Activity

(A) His6-Myc9-Net1 (lane 2) or a control sample from mock-infected cells (lane 1) purified in parallel was added to a standard transcription reaction that employed a linearized plasmid template that contained rDNA linked to its full promoter (extending to -210) as the template and 10–15 nM Pol I (Keener et al., 1998). An arrow indicates the position of [<sup>32</sup>P]-labeled runoff transcripts.

(B) Net1 enriched to >90% purity (Experimental Procedures) was fractionated by SDS-PAGE and stained with Coomassie Blue. M refers to molecular weight markers.

(C and D) Net1 stimulates Pol I activity. Dilution buffer (lanes 1 and 5) or increasing amounts of Net1 (lanes 2 to 4) were added to the transcription reaction. Quantitation of the amount of transcripts (arrow in C) as a function of Net1 concentration is plotted in (D).

phenylindole dihydrochloride (DAPI) staining, the majority (93%) of *net1-1* cells possessed more condensed rDNA semicircles that abutted directly against the DAPI-stained material (Figure 3F, compare rows 1 and 3). *net1* $\Delta$  cells did not arrest well in nocodazole, but they showed similar rDNA morphology as *net1-1* (data not shown), suggesting that Net1 is not an essential determinant of the unusual chromatin structure observed for rDNA in FISH experiments. Thus, in *net1* mutants, localization patterns of multiple nucleolar antigens as well as rDNA morphology are altered, although rDNA still congregates into a structure distinct from the bulk DNA.

#### *net1* and *sir2* Mutations Have Distinct Effects on the Nucleolus

Sir2 plays an important role in the nucleolus by suppressing intrachromosomal recombination within the rDNA repeats and silencing transcription by Pol II (reviewed in Guarente, 2000). Because Net1 tethers Sir2 to rDNA (Straight et al., 1999), all of the phenotypes observed for *net1* could, in theory, have been caused by a loss of Sir2 function within the nucleolus. However, this is clearly not the case because *net1* cells had either distinct or more severe phenotypes than *sir2* $\Delta$  in all

assays that were conducted. First, unlike in *net1* mutants, accumulation of rRNA was normal in *sir2Δ* (Figure 2A). Second, A190, Nop1, Nop2, and Fpr3 displayed normal (or nearly normal) nucleolar localization patterns in *sir2Δ* (Figures 3A–3D). Third, rDNA in *sir2Δ* cells, as revealed by FISH, displayed considerable heterogeneity and seemed to be less compact than that in wild-type or *net1-1* cells (Figure 3F). Thus, Net1 and Sir2 regulated nucleolar structure and function in distinct ways.

#### The *TAB6-1* Allele of *CDC14* Bypasses *tem1Δ* and *cdc15Δ*

The pleiotropic defects of the nucleolus in *net1* mutants add a confounding twist to the RENT control hypothesis. We originally proposed that Tem1-dependent disassembly of the RENT complex and the subsequent release of Cdc14 from the nucleolus drive cells from mitosis to interphase. *tem1Δ* and *cdc15Δ* cells arrest in late mitosis, but the *net1-1* mutation (also known as *tab2-1* for *telophase arrest bypassed*) enables these cells to exit mitosis, presumably by allowing Cdc14 to escape the nucleolus (Shou et al., 1999). However, given the profound disruption of nucleolar structure in *net1-1* cells, it is also possible that displaced nucleolar proteins other than Cdc14 caused or contributed to the *tem1Δ* and *cdc15Δ* bypass phenotype.

To test the RENT control hypothesis rigorously, we sought to identify a mutant form of Cdc14 with reduced binding affinity for Net1. If our hypothesis is correct, two predictions can be made for this mutant: (1) Like *net1-1*, it should be a *tab* mutant, because both mutations should allow ectopic release of Cdc14 from the nucleolus. (2) The *tem1Δ* and *cdc15Δ* bypass phenotype should be dominant. Based on this reasoning, we tested dominant mutants recovered in our earlier *tab* screen and found that the dominant *TAB6-1* mutation demonstrated tight linkage to *CDC14* (zero recombinants in thirty spores tested). Importantly, cloned *CDC14* sequence amplified from *TAB6-1*, but not wild-type cells, allowed bypass of *tem1Δ* (Figure 6A), confirming that *TAB6-1* is allelic to *CDC14*. The *TAB6-1* allele contained a Pro (116) → Leu mutation in *CDC14* (Figure 6B). Pro116 is conserved in Cdc14 homologs in *Drosophila* and *S. pombe* (CG7134 and SPAC1782.09c, respectively; Figure 6B), but not in *C. elegans*, *M. musculus*, or *H. sapiens*.

#### Cdc14<sup>TAB6</sup> Has Reduced Affinity for Net1, which Renders Clb5 Essential for Spore Viability

To interpret the phenotype of *TAB6-1* cells properly, it is important to understand the molecular mechanism by which *TAB6-1* bypassed *tem1Δ* and *cdc15Δ*. In *net1-1* mutants, bypass of the anaphase arrest that normally occurs upon depletion of Tem1 is accompanied by ectopic Clb2 degradation and Sic1 accumulation (Shou et al., 1999). *TAB6-1* cells behaved similarly to *net1-1* cells upon depletion of Tem1 (Figure 6C, compare lanes 8–14 [*TAB6-1*] with lanes 1–7 [+]). Moreover, like *net1-1*, *TAB6-1* bypassed anaphase arrest in almost all cells, since Clb2 degradation proceeded to near completion in Tem1-depleted cells (Figure 6C). We conclude that *net1-1* and *TAB6-1* most likely bypassed *cdc15Δ* by related mechanisms. To address whether *TAB6-1*, like *net1-1*, compromised the stability of RENT, we evaluated the Net1 binding and enzymatic activity of Cdc14

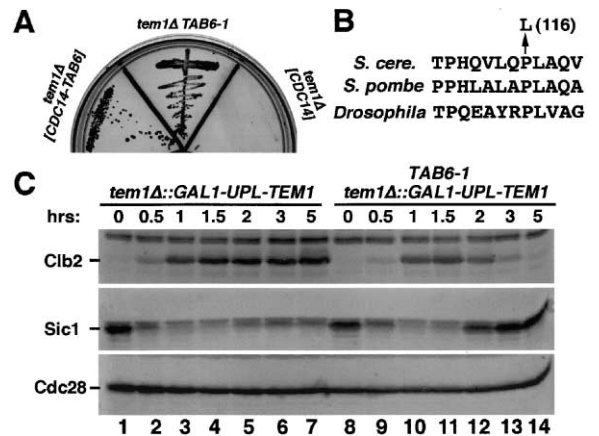


Figure 6. *TAB6-1* Is an Allele of *CDC14* that Bypasses *tem1Δ*  
(A) *TAB6-1* is an allele of *CDC14*. *tem1Δ::TRP1* [*GAL-TEM1/URA3*] *TAB6-1* cells (center), or *tem1Δ::TRP1* [*GAL-TEM1/URA3*] cells transformed with a *HIS3*-marked plasmid harboring *CDC14* derived from either wild type cells (right), or *TAB6* cells (left) were grown on YP galactose (YPG, *TEM1* expressed) and then plated on synthetic glucose medium containing 5-FOA to select for colonies that had lost the [*GAL-TEM1/URA3*] plasmid. After ten days at room temperature, the plate was photographed.

(B) *TAB6-1* has a single point mutation P116 → L. Cdc14 sequences flanking this amino acid from *S. cerevisiae*, *S. pombe*, and *Drosophila* are aligned.

(C) *TAB6-1* bypass of *tem1Δ* is accompanied by Clb2 degradation and Sic1 accumulation. Cells of the indicated genotypes grown in YPG (*TEM1* expressed) at 25°C were arrested in G1 phase with  $\alpha$  factor, and released into YP glucose (*TEM1* repressed) at time = 0. One and a half hours later,  $\alpha$  factor was added back to prevent cells from proceeding through a second cell cycle. At the indicated times, samples were taken to measure Clb2, Sic1, and Cdc28 protein levels by immunoblotting.

and Cdc14<sup>TAB6</sup>. Whereas purified Cdc14<sup>TAB6</sup> had nearly wild-type levels of phosphatase activity toward p-nitrophenyl phosphate and tyrosine-phosphorylated myelin basic protein (Figure 7A), it was bound less efficiently (Figure 7C) and was ~14-fold less sensitive to inhibition (Figure 7B) by a purified N-terminal fragment (amino acids 1–600) of Net1, which has been shown to bind and inhibit Cdc14 (Traverso et al., 2001). Similarly, Cdc14<sup>TAB6</sup>, but not Sir2, was less efficiently recovered in association with Myc9-Net1 upon immunoprecipitation of the RENT complex from yeast cell extracts (Figure 7D). These data imply that the P116L substitution allowed bypass of *cdc15Δ* and *tem1Δ* by reducing the affinity of Cdc14<sup>TAB6</sup> for Net1.

Unexpectedly, *TAB6-1* cells grew robustly at 25°C (Figure 7E), even though loss of temporal control over Cdc14 activity would be expected to perturb cell division and growth. Interestingly, whereas *TAB6-1 clb2Δ* cells were viable, *TAB6-1 clb5Δ* spores failed to form colonies (Figure 7F), suggesting that in the absence of the opposing activity of Clb5/Cdc28 (Shirayama et al., 1999), proper control of Cdc14 becomes essential for spore viability.

#### Cell Cycle Control and Nucleolar Functions of RENT Complex Can Be Uncoupled by the *TAB6-1* Allele of *CDC14*

Whereas both the *net1-1* and *TAB6-1* mutations destabilized the RENT complex and efficiently bypassed *tem1Δ*,

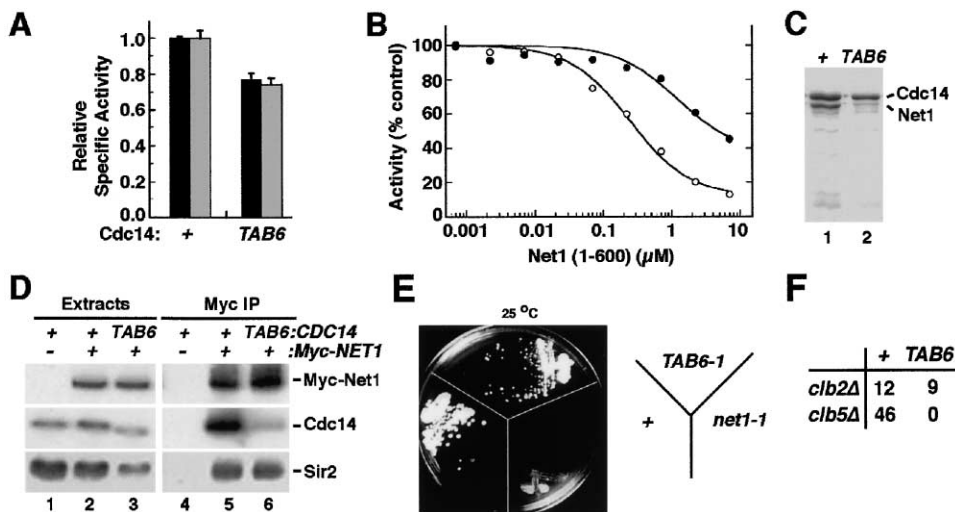


Figure 7. Cdc14<sup>TAB6</sup> Has Reduced Affinity for Net1, which Renders Clb5 Essential for Spore Viability

(A) Cdc14<sup>TAB6</sup> is nearly as active as Cdc14. The relative specific activities ( $\pm$  standard deviation,  $n = 3$ ) of purified GST-Cdc14 and GST-Cdc14<sup>TAB6</sup> were determined using the artificial substrates *p*-nitrophenyl phosphate (black bars) and tyrosine-phosphorylated myelin basic protein (Tyr-P-MBP) (gray bars).

(B) GST-Cdc14<sup>TAB6</sup> is less sensitive to inhibition by Net1(1-600). The activity of GST-Cdc14 (open circles) and GST-Cdc14<sup>TAB6</sup> (closed circles) was measured with 4  $\mu$ M Tyr-P-MBP in the presence of the indicated concentrations of purified Net1(1-600)-His<sub>6</sub>. The IC<sub>50</sub> values for Cdc14 and Cdc14<sup>TAB6</sup> are  $\sim$ 0.35 and 5  $\mu$ M, respectively.

(C) The affinity of Cdc14<sup>TAB6</sup> for Net1 is greatly reduced in vitro. Affinity matrices containing GST-Cdc14 (lane 1) and GST-Cdc14<sup>TAB6</sup> (lane 2) were mixed with a 4-fold molar excess of Net1(1-600)-His<sub>6</sub>. Proteins bound to the matrices were resolved by SDS-PAGE and stained with Coomassie Blue.

(D) *TAB6-1* selectively disengages Cdc14<sup>TAB6</sup> from the RENT complex. Extracts prepared from *NET1* (lanes 1 and 4), *MYC9-NET1* (lanes 2 and 5), and *MYC9-NET1 TAB6-1* (lanes 3 and 6) strains were immunoprecipitated with 9E10 antibodies. The input extracts (lanes 1–3) and immunoprecipitates (lanes 4–6) were immunoblotted with 9E10,  $\alpha$ -Cdc14, and  $\alpha$ -Sir2 antibodies as indicated.

(E) *TAB6-1* cells grow much better than *net1-1* cells at 25°C. Wild-type, *TAB6-1*, and *net1-1* cells were struck out on a YPD plate and allowed to grow at 25°C for 2.5 days before the photograph was taken.

(F) *TAB6-1 clb5Δ* (but not *TAB6-1 clb2Δ*) spores fail to survive. *clb2Δ::LEU2 CDC14/HIS3* and *clb5Δ::URA3 CDC14/HIS3* strains were mated with *TAB6-1*, and the diploid strains were dissected. The number of viable spores of the indicated genotypes were tabulated. Although *clb5Δ* (Chromosome XVI) and *TAB6-1* (chromosome VI) are unlinked, *clb5Δ TAB6-1* recombinants were never recovered.

*TAB6-1* cells grow much better than *net1-1* cells (Figure 7E). *CDC14<sup>TAB6</sup>* cells appeared to have a normal nucleolus by three distinct criteria: The localization patterns of A190, Nop1, Nop2, and Fpr3 (Figures 3A–3D), the morphology of rDNA (Figure 3F), and the levels of rRNA accumulation (Figure 2A) were all indistinguishable in *TAB6-1* and wild-type cells. These observations imply that regulation of nucleolar processes by Net1 was important for normal rates of cell growth, that bypass of *cdc15Δ* and *tem1Δ* by *TAB6-1* was not sustained by a general perturbation of nucleolar structure, and that ectopic release of Cdc14 from the nucleolus was sufficient for bypass. These data further imply that the nucleolar defects of *net1* mutants were not caused by weakened interaction between Net1 and Cdc14. Thus, *CDC14<sup>TAB6-1</sup>* uncoupled the cell cycle and nucleolar functions of the RENT complex by affecting the former without interfering with the latter.

## Discussion

### The Net1 Subunit of RENT Complex Directly Stimulates Transcription by Pol I

The RENT complex, consisting of at least three proteins (Net1, Cdc14, and Sir2), controls mitotic exit, mediates nucleolar silencing, and sustains proper localization of Nop1 (Shou et al., 1999; Straight et al., 1999; Visintin

et al., 1999). The first two functions of RENT are well documented and derive from the ability of Net1 to tether both Cdc14 and Sir2 to the nucleolus, respectively. Besides these phenotypes, we show here that *net1* mutants also exhibit delocalization of the A190 subunit of Pol I, a decreased rate of rRNA synthesis, and a reduced level of rRNA accumulation. The role of Net1 in Pol I-dependent rDNA expression is likely to be distinct from the nucleolar silencing and cell cycle control functions of RENT because *cdc14<sup>ts</sup>* and *sir2Δ* mutants do not exhibit defects in accumulation of rRNA. A simple model accommodating our data is that Net1 promotes expression of rDNA by helping to tether Pol I within the nucleolus. This hypothesis is supported by three lines of evidence. First, a Pol I subunit coimmunoprecipitates with Net1 from cell extracts. Second, purified Net1 binds purified Pol I in vitro and stimulates its activity at near equimolar ratio. Third, a *CEN/ARS* plasmid expressing *Arn3*, a recruitment factor for Pol I promoter, is sufficient to suppress the *ts* growth defect of both *net1-1* and *net1Δ*. A more detailed mechanistic understanding of how Net1 promotes Pol I action awaits further biochemical studies.

### Role of Net1 in Global Nucleolar Structure

Two proteins (Sir2 and Cdc14) and one protein complex (Pol I) that bind directly to Net1 are delocalized in *net1*

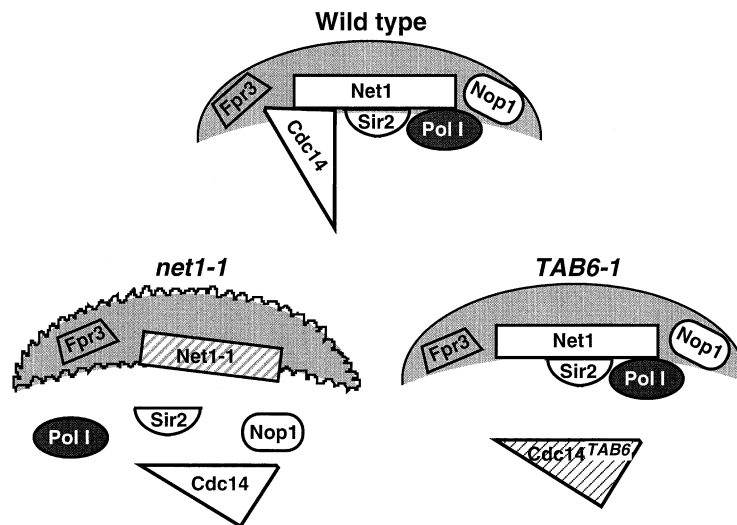


Figure 8. *TAB6-1* Uncouples the Nucleolar and Cell Cycle Functions of RENT  
See Discussion for details.

Phenotypes:

- bypass of *tem1Δ* and *cdc15Δ*
- defective nucleolar silencing
- defective rDNA morphology
- delocalized rRNA processing factors
- diminished Pol I function

bypass of *tem1Δ* and *cdc15Δ*

mutants. However, Nop1, which does not bind stably to Net1, is also delocalized in *net1* mutant cells. One explanation comes from the observation that the nucleolar localization of rRNA processing factors Nop1 and Gar1 is reduced upon inhibition of transcription of rDNA (Trumtel et al., 2000). Thus, Nop1 and Nop2, both involved in rRNA processing (Tollervey et al., 1993; Hong et al., 1997), may become delocalized in *net1Δ* mutants in part due to decreased synthesis of rRNA. Supporting this proposal, *RRN3* suppression of *net1*, presumably involving stimulation of Pol I transcription (Yamamoto et al., 1996; Keener et al., 1998), correlates with partial restoration of Nop1 nucleolar localization (Figure 1D). An alternative possibility is suggested by the recent report that Pol I holoenzyme, some of its transcription activators, and rRNA processing factors assemble together into a functional supercomplex whose integrity does not depend on rRNA transcription by Pol I (Fath et al., 2000). Our observation that *net1* mutations lead to simultaneous loss of Pol I and rRNA processing components (Nop1, Nop2) from the nucleolus raises the possibility that Net1 contributes to either the integrity or the nucleolar anchorage of the supercomplex.

Intriguingly, in *net1* cells, the nucleolar protein Fpr3 retains a focal, albeit more compact, localization resembling the morphology of *net1-1* rDNA. A similar compaction has been reported for the “nucleolar remnant” visualized by electron microscopy upon thermal inactivation of RNA Pol I (Trumtel et al., 2000). Thus, we suggest that congregation of rDNA repeats occurs even in the absence of Net1 and that Fpr3 is recruited to the nucleolus by a Net1- and transcription-independent pathway.

Although the nucleolar defects of *net1* cells are likely to arise in part due to diminished Pol I activity and dispersion of Sir2, it seems probable that Net1 serves additional functions within the nucleolus. This prediction is

based on four observations. First, the overall growth defect and thermosensitive phenotypes of *net1* mutants are partially corrected by *RRN3* but are not alleviated by ectopic expression of rDNA by Pol II at a level sufficient to support growth of cells lacking a subunit of Pol I (J. Claypool and W.S., data not shown). Second, chromatin IP experiments indicate that Net1 decorates the entire rDNA sequence and is not restricted to the promoter region (Straight et al., 1999). Indeed, Net1 still localized to the altered nucleolus in a *rrn5Δ PSW* (polymerase switched) strain in which Pol II instead of Pol I transcribed rDNA (I. Siddiqi, M. Oakes, and M.N., unpublished data; for PSW strains, see Oakes et al., 1999). These observations suggest that Net1 “coats” rDNA and regulates its structure in the presence or absence of the Pol I transcriptional machinery. Third, *rrn5Δ PSW* cells are viable when Pol I is inactivated but are inviable in combination with *net1Δ* (I. Siddiqi and M.N., unpublished results). Fourth, the morphologies of rDNA in *net1-1* and *sir2Δ*, as judged by FISH analysis, are clearly distinct, suggesting that *SIR2* alone can not account for *NET1* functions. On the other hand, a loss of Sir2 function may account for the perturbation of rDNA copy number control that we observed in *net1* mutants. Chromosome XII ran as a smear in *net1Δ* cells (W.S., J.D., and M. Oakes, unpublished results), possibly because of increased recombination among rDNA repeats upon delocalization of Sir2 (Gottlieb and Esposito, 1989).

***TAB6-1* Uncouples Nucleolar and Cell Cycle Functions of RENT Complex**

*net1-1* was originally isolated as a bypass suppressor of *cdc15Δ* and *tem1Δ*, presumably because it allows Cdc14 to be released from the nucleolus during anaphase in a Tem1/Cdc15-independent manner (Shou et al., 1999). However, the exact mechanism of bypass is

obscured by the pleiotropic nucleolar defects of the *net1-1* mutant. The possibility that the release of some nucleolar protein other than Cdc14 is responsible for *tem1* $\Delta$  bypass was instigated further by the observation that two other recessive *tab* mutants (*tab1*, *15D2*) exhibited defects in nucleolar integrity (K.S. and W.S., unpublished data). Furthermore, it is unclear whether the severe growth defect of *net1* $\Delta$  and *net1-1* (Shou et al., 1999; Straight et al., 1999) arises from loss of the cell cycle or nucleolar functions of Net1.

The identification of the *TAB6-1* allele of *CDC14* allowed us to begin to address how the cell cycle and nucleolar functions of RENT are related (Figure 8). Both *TAB6-1* and *net1-1* efficiently bypass cell cycle arrest in *Tem1*-depleted cells, presumably because free Cdc14 enables ectopic degradation of Clb2 and accumulation of Sic1. Unlike *net1-1* mutants, there are no obvious general defects in nucleolar organization or function in *TAB6-1* mutants, as judged by the localization patterns of Nop1, Nop2, Fpr3, and A190, the morphology of rDNA, the number of rDNA repeats (W.S. and J.D., data not shown), and the level of rRNA accumulation. Thus, the more severe growth phenotype observed in *net1* mutants is likely due to defective nucleolar functions rather than cell cycle functions. Furthermore, by affecting cell cycle functions without perturbing nucleolar functions of the RENT complex, *TAB6-1* confirms that release of Cdc14 from RENT is sufficient to trigger mitotic exit in *cdc15* $\Delta$  cells.

#### Experimental Procedures

##### Isolation of *RRN3* as a Low-Copy Suppressor of *net1-1*

The *net1-1* mutant strain was transformed with yeast genomic plasmid libraries and was incubated at 25°C for one day before being shifted to 37°C. Low-copy CEN/ARS-based libraries from the laboratories of P. Heiter (ATCC#77164) and R. Young (Thompson et al., 1993) yielded a *net1-1* complementing activity from chromosome XI, 206,300-210,665. Each open reading frame in this genomic region was amplified by polymerase chain reaction and tested for its ability to complement the temperature sensitivity of *net1-1*. The complementing activity resided in *RRN3*.

##### RNA Isolation and Northern Blot

Cells grown in 12 ml YPD at 23°C to an OD<sub>600</sub> of ~0.8 were shifted to 37°C for 3 hr. Cell pellets were resuspended in 1 ml buffer (50 mM sodium acetate, 10 mM EDTA, 0.1% sodium dodecyl sulfate [SDS]), and RNA was extracted with 1 ml of phenol, followed by 1 ml of phenol/chloroform (1:1) by incubation at 65°C for 4 min and on ice for 4 min. RNA was precipitated with ethanol, 5  $\mu$ g of which was fractionated on a 1.5% agarose gel containing formaldehyde, stained with ethidium bromide, and quantitated using the Alpha Image 2000 system. The actin probe in Northern blotting was generated by polymerase chain reaction using primers CCAATTGCTCGA GAGATTCT and AGTGATGACTTGACCATC. Random priming was performed with the Megaprime DNA labeling system (Amersham, Arlington Heights, IL). Quantitation was done on a Quantity One Phosphorimager (Bio-Rad, Hercules, CA).

##### Pulse-Chase Labeling of rRNA

Pulse-chase labeling and analysis of rRNA was carried out essentially as described (Udem and Warner, 1972; Warner, 1991; Powers and Walter, 1999). Briefly, cultures were grown in minimal medium lacking methionine or uracil at 25°C to OD<sub>600</sub> = 0.2–0.3, and incubated at 37°C for 3 hr. Cultures were adjusted to OD<sub>600</sub> = 0.4, pulse labeled with [<sup>3</sup>H<sub>3</sub>]-methionine (40  $\mu$ Ci/ml final) or [<sup>3</sup>H] uracil (22  $\mu$ Ci/ml final; New England Nuclear Life Sciences/Perkin Elmer Life Sciences, Boston, MA) for 5 min, and chased with unlabeled methio-

nine (3 mM final) or unlabeled uracil (0.3 mg/ml final), respectively, for various periods of time at 37°C; ~1.5 ml aliquots were taken for each sample, and RNA was extracted using hot phenol method and fractionated on a 6.7% formaldehyde-1.5% agarose gel. The gel was soaked in Enhance (DuPont, Wilmington, DE) overnight, vacuum dried, and exposed to film with an enhancer screen at -80°C. The intensity of the 25S bands was quantitated using the NIH Image 1.62b7 software.

##### Purification of Full-Length Net1 and In Vitro Transcription Assay

His6-Myc9-Net1 was expressed in Hi5 insect cells and purified using a nickel affinity column, as described (Shou and Dunphy, 1996). Eluted protein was dialyzed in 20 mM Buffer J (Tris-Cl [pH 7.9], 20% glycerol, 0.05% Tween-20, 1 mM dithiothreitol [DTT], 50 mM KCl), applied to a 1 ml SP-sepharose cartridge (Amersham Pharmacia, Piscataway, NJ), and eluted with a 48 ml salt gradient from 50 mM to 1 M KCl in Buffer J at 0.25 ml/min. Peak fractions (at ~200 mM KCl) were applied to a 1 ml Q-sepharose cartridge (Amersham Pharmacia) and eluted with a 9 ml salt gradient from 50 mM to 1 M KCl in Buffer J at 0.25 ml/min. Peak fractions (at ~300 mM KCl) were concentrated approximately 4-fold using a Microcon 30 concentrator (Amicon/Millipore, Bedford, MA) and assayed for activity. In vitro transcription was carried out essentially as described previously (Keener et al., 1998). Present in all the reactions were 0.2–0.4 nM wild-type linear template (extending 210 bp upstream of the +1 start site), Rm3 (2–6 nM)-Pol I (10–15 nM) complex, and much smaller amounts of UAF, TBP, and CF (Keener et al., 1998).

##### Purification and Analysis of Net1(1-600), Cdc14, and Cdc14<sup>TAB6</sup>

GST-Cdc14 and GST-Cdc14<sup>TAB6</sup> were purified from *E. coli* using glutathione-Sepharose beads, and Net1(1-600)-His<sub>6</sub> was purified from *E. coli* on His-bind resin (Novagen, Madison, WI; Traverso et al., 2001). Phosphatase assays were performed in buffer P (50 mM imidazole [pH 6.8], 1 mM EDTA, 1 mM DTT, 0.5 mg/ml bovine serum albumin) at 30°C using 20 mM *p*-nitrophenyl phosphate or 4  $\mu$ M myelin basic protein phosphorylated on tyrosines (Tyr-P-MBP; Taylor et al., 1997). The ability of purified Net1(1-600)-His<sub>6</sub> to inhibit GST-Cdc14 and GST-Cdc14<sup>TAB6</sup> was assessed in phosphatase assays performed at 30°C with 10 nM enzyme and 4  $\mu$ M Tyr-P-MBP in buffer P containing 120 mM KCl.

One nmol of Net1(1-600)-His<sub>6</sub> was added to glutathione-Sepharose beads containing 0.25 nmol of GST-Cdc14 or GST-Cdc14<sup>TAB6</sup> in 1 ml buffer B (25 mM Tris [pH 7.4], 137 mM NaCl, 2.6 mM KCl, 0.1% 2-mercaptoethanol). The mixture was mixed for 30 min at 4°C and washed four times with 1 ml buffer B + 0.01% Triton X-100. Aliquots (20  $\mu$ l) of washed beads were separated on a 12% SDS-polyacrylamide gel and stained with Coomassie Blue.

##### Other Methods

The in vitro binding assay of Net1 and Pol I was performed at 4°C: 40  $\mu$ l of Protein A sepharose beads (Sigma, St. Louis, MO, USA) were washed with Buffer R (20 mM HEPES/KOH [pH 7.5], 150 mM NaCl, 0.2% Triton X-100, 1 mM DTT) and then incubated with 2  $\mu$ l of 12CA5 anti-HA ascites in Buffer A (20 mM HEPES/KOH [pH 7.5], 150 mM NaCl, 0.1 mg/ml BSA, 2 mM EDTA, 1 mM DTT) for 1 hr. After incubation, beads were washed six times with Buffer R and one time with Buffer A and were split into two 20  $\mu$ l aliquots; 150 ng of purified Pol I, either HA tagged at the A135 subunit or untagged, in Buffer A was added to each aliquot, respectively, and the beads were incubated for 1 hr. After incubation, the beads were washed six times with Buffer R and one time with Buffer A; 150 ng of Myc9-Net1 purified from insect cells was added to each aliquot and incubated for an additional hour. The beads were washed ten times with Buffer R and two times with Buffer A. Twenty microliters of 2  $\times$  SDS sample buffer was added to each aliquot and boiled, and 9  $\mu$ l was loaded on an 8% SDS-polyacrylamide gel electrophoresis (SDS-PAGE) gel for further analysis.

Other procedures were described previously (Shou et al., 1999). For Western blots, primary antibodies were as follows: 1:2K  $\alpha$ -A190, 1:2.5K  $\alpha$ -Sir2, 1:5K  $\alpha$ -Nop1, 1:2K 9E10, 1:2.5K  $\alpha$ -Clb2, 1:8K  $\alpha$ -Sic1, 1:6K  $\alpha$ -Cdc28, and 1:1K  $\alpha$ -Cdc14. For immunofluorescence, cells were fixed with 4.5% formaldehyde at room temperature for 0.5 hr for all primary antibodies, which included 1:1K rabbit  $\alpha$ -A190, 1:12K

mouse  $\alpha$ -Nop1, 1;1K 9E10 (Babco/CRP, Richmond, CA), and 1:200 rabbit  $\alpha$ -Cdc14. FISH analysis was carried out as previously described (Guacci et al., 1994).

#### Acknowledgments

This work was supported by a Beckman Foundation Young Investigator Award (to R.J.D.), National Institutes of Health grants GM59940 (to R.J.D.), GM35949 (to M.N.), CA59935 (to H.C.), and an Ellison Medical Foundation grant (to D.M.). We thank R. Verma, T. Powers, M. Oakes, J. Claypool, and B. Hay for discussions; D. Chan, W. Dunphy, B. Hay, H. Rao, R. Lipford, R. Verma, D. Mohl, and S. Schwarz for critical reading of the manuscript; H. Mountain, P. Philippsen, F. Cross, and M. Shirayama for strains and plasmids; D. Koshland and V. Guacci for FISH probes and protocols; C. Thompson for yeast genomic library; and J. Aris, J. Thorner, and D. Kellogg for antibodies. W.S. was an HHMI predoctoral fellow.

Received February 28, 2001; revised April 30, 2001.

#### References

- Benton, B.M., Zang, J.H., and Thorner, J. (1994). A novel FK506- and rapamycin-binding protein (FPR3 gene product) in the yeast *Saccharomyces cerevisiae* is a proline rotamase localized to the nucleolus. *J. Cell Biol.* **127**, 623–639.
- Cockell, M.M., and Gasser, S.M. (1999). The nucleolus: nucleolar space for RENT. *Curr. Biol.* **9**, R575–R576.
- de Beus, E., Brockenbrough, J.S., Hong, B., and Aris, J.P. (1994). Yeast NOP2 encodes an essential nucleolar protein with homology to a human proliferation marker. *J. Cell Biol.* **127**, 1799–1813.
- Fath, S., Milkereit, P., Podtelejnikov, A.V., Bischler, N., Schultz, P., Bier, M., Mann, M., and Tschochner, H. (2000). Association of yeast RNA polymerase I with a nucleolar substructure active in rRNA synthesis and processing. *J. Cell Biol.* **149**, 575–590.
- Garcia, S.N., and Pillus, L. (1999). Net results of nucleolar dynamics. *Cell* **97**, 825–828.
- Gottlieb, S., and Esposito, R.E. (1989). A new role for a yeast transcriptional silencer gene, SIR2, in regulation of recombination in ribosomal DNA. *Cell* **56**, 771–776.
- Gottschling, D.E. (2000). Gene silencing: two faces of SIR2. *Curr. Biol.* **10**, R708–R711.
- Gruneberg, U., Campbell, K., Simpson, C., Grindlay, J., and Schiebel, E. (2000). Nud1p links astral microtubule organization and the control of exit from mitosis. *EMBO J.* **19**, 6475–6488.
- Guacci, V., Hogan, E., and Koshland, D. (1994). Chromosome condensation and sister chromatid pairing in budding yeast. *J. Cell Biol.* **125**, 517–530.
- Guarente, L. (2000). Sir2 links chromatin silencing, metabolism, and aging. *Genes Dev.* **14**, 1021–1026.
- Hong, B., Brockenbrough, J.S., Wu, P., and Aris, J.P. (1997). Nop2p is required for pre-rRNA processing and 60S ribosome subunit synthesis in yeast. *Mol. Cell. Biol.* **17**, 378–388.
- Jaspersen, S.L., Charles, J.F., and Morgan, D.O. (1999). Inhibitory phosphorylation of the APC regulator Hct1 is controlled by the kinase Cdc28 and the phosphatase Cdc14. *Curr. Biol.* **9**, 227–236.
- Keener, J., Josaitis, C.A., Dodd, J.A., and Nomura, M. (1998). Reconstitution of yeast RNA polymerase I transcription in vitro from purified components: TATA-binding protein is not required for basal transcription. *J. Biol. Chem.* **273**, 33795–33802.
- Morgan, D.O. (1999). Regulation of the APC and the exit from mitosis. *Nat. Cell Biol.* **1**, E47–E53.
- Oakes, M., Siddiqi, I., Vu, L., Aris, J., and Nomura, M. (1999). Transcription factor UAF, expansion and contraction of ribosomal DNA (rDNA) repeats, and RNA polymerase switch in transcription of yeast rDNA. *Mol. Cell. Biol.* **19**, 8559–8569.
- Powers, T., and Walter, P. (1999). Regulation of ribosome biogenesis by the rapamycin-sensitive TOR-signaling pathway in *Saccharomyces cerevisiae*. *Mol. Biol. Cell* **10**, 987–1000.
- Shaw, P.J., and Jordan, E.G. (1995). The nucleolus. *Annu. Rev. Cell Dev. Biol.* **11**, 93–121.
- Shirayama, M., Toth, A., Galova, M., and Nasmyth, K. (1999). APC(Cdc20) promotes exit from mitosis by destroying the anaphase inhibitor Pds1 and cyclin Clb5. *Nature* **402**, 203–207.
- Shou, W., and Dunphy, W.G. (1996). Cell cycle control by *Xenopus* p28Kix1, a developmentally regulated inhibitor of cyclin-dependent kinases. *Mol. Biol. Cell* **7**, 457–469.
- Shou, W., Seol, J.H., Shevchenko, A., Baskerville, C., Moazed, D., Chen, Z.W., Jang, J., Shevchenko, A., Charbonneau, H., and Deshaies, R.J. (1999). Exit from mitosis is triggered by Tem1-dependent release of the protein phosphatase Cdc14 from nucleolar RENT complex. *Cell* **97**, 233–244.
- Straight, A.F., Shou, W., Dowd, G.J., Turck, C.W., Deshaies, R.J., Johnson, A.D., and Moazed, D. (1999). Net1, a Sir2-associated nucleolar protein required for rDNA silencing and nucleolar integrity. *Cell* **97**, 245–256.
- Tanner, K.G., Landry, J., Sternglanz, R., and Denu, J.M. (2000). Silent information regulator 2 family of NAD-dependent histone/protein deacetylases generates a unique product, 1-O-acetyl-ADP-ribose. *Proc. Natl. Acad. Sci. USA* **97**, 14178–14182.
- Tanny, J.C., and Moazed, D. (2000). Coupling of histone deacetylation to NAD breakdown by the yeast silencing protein Sir2: evidence for acetyl transfer from substrate to an NAD breakdown product. *Proc. Natl. Acad. Sci. USA* **98**, 415–420.
- Taylor, G.S., Liu, Y., Baskerville, C., and Charbonneau, H. (1997). The activity of Cdc14p, an oligomeric dual specificity protein phosphatase from *Saccharomyces cerevisiae*, is required for cell cycle progression. *J. Biol. Chem.* **272**, 24054–24063.
- Thompson, C.M., Koleske, A.J., Chao, D.M., and Young, R.A. (1993). A multisubunit complex associated with the RNA polymerase II CTD and TATA-binding protein in yeast. *Cell* **73**, 1361–1375.
- Tollervey, D., Lehtonen, H., Jansen, R., Kern, H., and Hurt, E.C. (1993). Temperature-sensitive mutations demonstrate roles for yeast fibrillar in pre-rRNA processing, pre-rRNA methylation, and ribosome assembly. *Cell* **72**, 443–457.
- Traverso, E.E., Baskerville, C., Liu, Y., Shou, W., James, P., Deshaies, R.J., and Charbonneau, H. (2001). Characterization of the Net1 cell cycle-dependent regulator of the Cdc14 phosphatase from budding yeast. *J. Biol. Chem.* **276**, 21924–21931.
- Trumtel, S., Leger, S.I., Gleizes, P.E., Teulier, F., and Gas, N. (2000). Assembly and functional organization of the nucleolus: ultrastructural analysis of *Saccharomyces cerevisiae* mutants. *Mol. Biol. Cell* **11**, 2175–2189.
- Udem, S.A., and Warner, J.R. (1972). Ribosomal RNA synthesis in *Saccharomyces cerevisiae*. *J. Mol. Biol.* **65**, 227–242.
- Visintin, R., Craig, K., Hwang, E.S., Prinz, S., Tyers, M., and Amon, A. (1998). The phosphatase Cdc14 triggers mitotic exit by reversal of Cdk-dependent phosphorylation. *Mol. Cell* **2**, 709–718.
- Visintin, R., Hwang, E.S., and Amon, A. (1999). Cfi1 prevents premature exit from mitosis by anchoring Cdc14 phosphatase in the nucleolus. *Nature* **398**, 818–823.
- Warner, J.R. (1991). Labeling of RNA and phosphoproteins in *Saccharomyces cerevisiae*. *Methods Enzymol.* **194**, 423–428.
- Yamamoto, R.T., Nogi, Y., Dodd, J.A., and Nomura, M. (1996). RRN3 gene of *Saccharomyces cerevisiae* encodes an essential RNA polymerase I transcription factor which interacts with the polymerase independently of DNA template. *EMBO J.* **15**, 3964–3973.
- Zachariae, W., and Nasmyth, K. (1999). Whose end is destruction: cell division and the anaphase-promoting complex. *Genes Dev.* **13**, 2039–2058.